Subpicosecond pump–probe measurements of the electronic relaxation rates of the S_1 states of azulene and related compounds in polar and nonpolar solvents

Brian D. Wagner, Marian Szymanski, and Ronald P. Steer
Department of Chemistry, University of Saskatchewan, Saskatoon, Saskatchewan, Canada, S7N 0W0

(Received 7 August 1992; accepted 22 September 1992)

The lifetimes of the S_1 states of azulene, azulene-d_8, 4,6,8-trimethylazulene, and guaiazulene (1,4-dimethyl-7-isopropylazulene) have been measured in three nonviscous solvents of different polarity and structure using a two-photon, two-color, pump–probe method with subpicosecond time resolution. A significant solvent effect is measured. The rate constants for $S_1 \rightsquigarrow S_0$ internal conversion in all four compounds in all three solvents exhibit one common S_1–S_0 energy gap law correlation, indicating that variations in the electronic relaxation rates are governed exclusively by changes in the Franck–Condon factors for the transition. No effect is observed when the exciting wavelength is changed, indicating that vibrational relaxation is occurring on a time scale which is faster than that of electronic relaxation in these systems. No significant deuterium isotope effect is measured in azulene, indicating that high frequency C–H(D) stretching vibrations do not act as significant accepting modes in the radiationless transition.

I. INTRODUCTION

Interest in the dynamic behavior of the electronically-excited, valence-shell states of nonalternant aromatic hydrocarbons has remained high since the discovery of azulene's "anomalous" $S_2 \rightarrow S_0$ fluorescence nearly four decades ago.[1,2] Emission-based methods have proved most convenient for studying the relaxation of the S_2 states of these compounds, and have been employed in recent reexaminations of the behavior of azulene and some of its simple derivatives in both supersonic jets[3,4] and in liquid solution.[5] However, the S_1 states are almost nonfluorescent ($\phi_f \sim 10^{-6}$),[6] and the electronic structures and dynamics of these lower excited states must therefore be deduced from pump–probe, optical–optical double resonance, absorption linewidth and other such measurements. Pump–probe methods have been employed most frequently in the dynamics studies, and recent advances in femtosecond laser technology[7] have greatly improved the time resolution which such experiments afford.

Despite the widespread attention which has been focused on the S_1 states of azulene and related systems, a surprisingly large number of questions about them remain unresolved. First, substantial differences exist among the reported lifetimes of the S_1 state of the parent compound.[6,8–18] Many of these measurements have been made in different media, using different excitation wavelengths. However, even those measurements made under ostensibly the same conditions have not yielded lifetimes which are the same within stated experimental errors. Consider, for example, the recent measurement by Schwarzer *et al.*[17] of τ $(S_1) = 1.0 \pm 0.1$ ps for azulene excited at 613 nm in cyclohexane at room temperature compared with the long-accepted value of 1.9 ± 0.2 ps measured by Ippen *et al.*[12,13] under almost identical conditions. Second, the effect of the medium on the rate (and "mechanism") of electronic relaxation remains uncertain. Lifetimes of the S_1 state of isolated azulene as a function of vibrational energy content have been calculated from absorption linewidth measurements in supersonic expansions,[14–16] and range from 1.1 or 1.0 or 0.8 ps in the zero point level to 0.3 ps at $E_{\text{vib}} = 2417$ cm^{-1}. Embedding azulene in a liquid solvent is known to result in very rapid vibrational relaxation of the excited solute.[17,18] However, the measured lifetimes of vibrationally relaxed S_1 azulene, in condensed media show no consistent trend. Thus, although Drent *et al.*[8] originally reported a solvent heavy atom effect, no such effect was observed by Ippen and co-workers[12,13] who examined azulene in cyclohexane, benzene, benzene-d_6, chlorobenzene, and bromobenzene. Schwarzer *et al.*[17] also observed no effect on replacing cyclohexane by 1,1,2-trichlorotrifluoroethane, but obtained a significantly smaller value of τ (S_1) than Ippen and Shank.[12,13] On the other hand Matsumoto *et al.*[18] have suggested that the difference between their measured S_1 electronic relaxation time (3.0 ps) and the lower values of others could be attributed to the high viscosity and/or dielectric constant of their host medium, ethylene glycol. To our knowledge a systematic study of the effect of solvent structure and solvent–solute interaction energy on the electronic relaxation rates of azulene and related compounds has not been undertaken. The intriguing question of the possible involvement of intermolecular, medium-induced perturbations in the relaxation of the S_1 state of azulene[14] has also not yet been satisfactorily addressed.

Finally, the details of the intramolecular interactions which are responsible for the anomalously short lifetimes of the S_1 states of azulene and related nonalternant hydrocarbons remain largely unknown. The absence of a significant deuterium isotope effect on S_1's radiationless decay rate in solution,[13,17] and the large changes in the structure of the carbon skeleton on $S_1 \leftarrow S_0$ excitation[15] suggest qualitatively that low frequency C–C stretching and C–C–C

0021-9606/93/010301-7$06.00
© 1993 American Institute of Physics

bending rather than high frequency in-plane C–H(D) stretching vibrations are the primary accepting modes in the intramolecular radiationless decay.[19] However, the frequencies of many optically inactive low frequency modes of the S_1 and S_2 states azulene are unknown,[15] and detailed calculations of the complete set of Franck–Condon factors for the $S_2 \rightsquigarrow S_0^v$ and $S_2 \rightsquigarrow S_1^v$ processes have therefore not been possible.

In this paper we employ fast time-resolved, pump–probe methods to re-examine the dynamics of the S_1 states of azulene and some of its simple derivatives in solution. We assess the effect of solvent and excitation wavelength on their electronic relaxation rates and thus provide information which will be of use in formulating a more satisfactory model for $S_1 \rightsquigarrow S_0$ internal conversion in these compounds.

II. EXPERIMENTAL DETAILS

Azulene (AZ) and guaiazulene (GAZ, 1,4-dimethyl-7-isopropyl-azulene), both from Aldrich, were used as received. Azulene-d_8 (AZ-d_8) was kindly supplied by Professor B. Nickel. 4,6,8-trimethylazulene (TMA) was synthesized and purified according to the method of Garst *et al.*[20] The laser dyes DCM, pyridine-1, and αNPO (Exciton) were used as received. Acetonitrile and 1,1,2-trichlorotrifluoroethane (MeCN and TCE; both BDH Ominisolv) were used as received. Cyclohexane (CH; BDH Omnisolv) was fractionally distilled before use. S_1 energies were determined from the wavelengths of the 0–0 bands in the absorption spectra in each solvent.

The experimental set-up for the pump–probe measurements is shown schematically in Fig. 1. (The sources of the various commercially available components are given in the figure caption.) The output (light-stabilized mode) of a mode-locked Nd:YAG laser (15 W) is passed through a fiberoptic infrared (IR) pulse compressor[21] and a second-harmonic generating crystal, and is stabilized via an acousto-optic feedback loop, yielding a train of stabilized 532 nm pulses, with an average full temporal width at half-maximum (FWHM) of ~2.5 ps and an average power of 1.0 W. This output is split into two beams of equal intensity which are used to synchronously pump two fs dye lasers, one using DCM dye (the pump), the other using pyridine-1 (the probe). This arrangement permits the wavelengths of the pump and probe lasers to be varied independently, albeit at the expense of some time resolution in the system. Each dye laser produces between 70 and 100 mW of average power, depending on the wavelength. The output pulses have a sech^2 shape, with a FWHM of 0.4–0.6 ps as measured by the autocorrelation technique.[22] The experiment is located on a floating table (Newport), to isolate the system from external vibrations and hence reduce the relative temporal jitter between the two trains of dye laser pulses.

The pump beam is passed through an optical delay line, consisting of a fixed mirrored right-angle prism, and a mirror retroreflector mounted on a motor-driven translation stage which has a 25 mm range. This arrangement provides a maximum delay time of 166 ps. The probe beam is passed through a polarization rotator consisting of a fresnel double rhomb mounted on a motor-driven 360° rotation stage, in order to control angle between the planes of polarization of the pump and probe beams. Both the translation and rotation stages are under computer control.

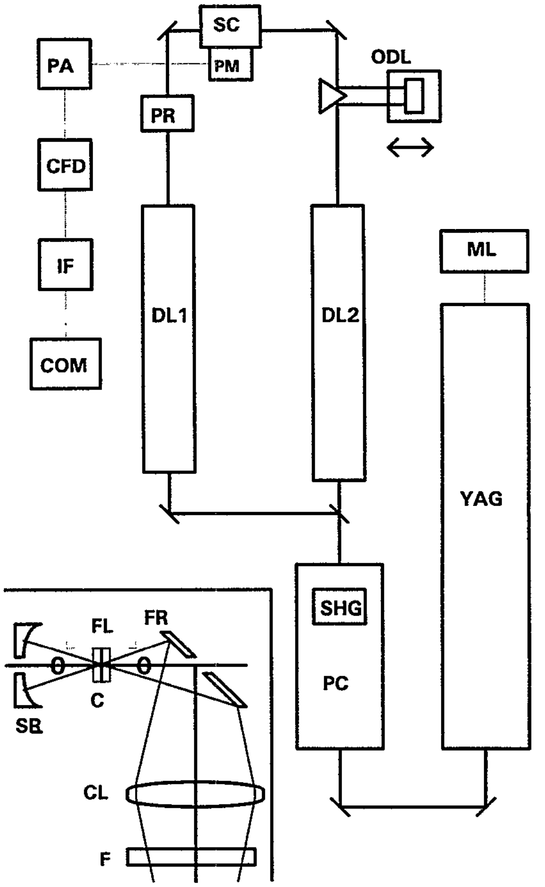

FIG. 1. Schematic diagram of the experimental set-up. YAG, Spectra Physics (SP) model 3800S Nd:YAG laser; ML, SP model 3242 41 MHz mode locker; PC, SP model 3695 IR pulse compressor; SHG, SP model 3225 second harmonic generation assembly; DL1, DL2, SP model 3510 fs dye lasers; PR, polarization rotator consisting of a Continental Optical model FRD-42 fresnel double rhomb prism mounted in a Klinger model UR100CC dc motor driven 360° rotation stage; ODL, optical delay line consisting of a fixed mirrored right-angle prism and a Newport model BBR1-5 retroreflector mounted on a Klinger model UT100CC dc motor driven 25 mm translation stage; PM, Hamamatsu model R928 photomultiplier tube; PA, preamplifier; CFD, Ortec model 473A constant fraction discriminator; IF, Stanford Research model SR245 IEEE-488 computer interface; COM, computer; SC, sample chamber. (Inset) The optical configuration of the sample chamber. SR, 60 mm diam, 50 mm radius spherical reflector; C, 0.1 or 0.2 mm path length quartz cell; FR, 60 mm diam flat reflector; CL, 63 mm diam, 50 mm focal length condensing lens; FL, 3 mm diam, 1 in. focal length lenses. Both reflectors have 2 mm diam holes drilled through their centers (at a 45° angle in the case of the flat reflector) and special coatings which are transmissive in the dye laser wavelength region (500–800 nm) and highly reflective in the fluorescence wavelength region (300–500 nm), and were custom made by Interoptics Ltd.

The pump and probe laser beams are collinearly counterpropagated into the sample chamber and are focused onto the sample (0.1 or 0.2 mm path length) using a pair of 3 mm diam, 1 in. focal length lenses. This gives a peak power density for each laser of ~1×10^5 W/cm^2 at the focus. The sample emission is collected by a spherical reflector (on the probe side) and a flat reflector (on the pump side) which direct the collected light through a focusing lens and a set of filters (to remove the fundamental laser wavelengths) to a photomultiplier tube (PMT) (cf. inset of Fig. 1). Both reflectors have 2 mm diam holes drilled through their centers, to allow passage of the laser beams. This configuration of the optics provides an emission collection solid angle of 10.5°. The PMT signal is passed through a preamplifier and a constant fraction discriminator. The resulting signal intensity is displayed as a count rate (cps) by a digital ratemeter, and is sent via an IEEE-488 interface to a computer for storage.

An experiment consists of moving the translation (or rotation) stage in appropriate increments, and collecting an average count rate at each stage position. In general, each recorded value is the average of 10 (or more) such individual readings, although if the intensity is low the single total of 10 readings may be used. Unlike other pump–probe experiments,[12,13,17] the pump and probe beams are not chopped and a lock-in amplifier is not used for signal to noise enhancement. In this way we ensure that the whole system remains stable over the course of an entire experiment. In these circumstances, however, considerable background is generated by one-beam, two-photon absorption. The scan range is chosen so as to give a good measure of this flat base line before and after the peak, in order to permit accurate background subtraction prior to data analysis.

Deconvolution of the instrument response function is required in order to recover the sample excited state lifetime from the intensity (cps) vs stage position data.[12] To do this, the cross-correlation function of the pump–probe system is measured using the ultraviolet (UV) laser dye αNPO, which has a significant two-photon absorption cross section and fluoresces from its S_1 state with $\lambda_{\max}=390$ nm. The instrument response curve is obtained by scanning a solution of αNPO in methanol under the same conditions and scan increment as the azulene sample. The deconvolution is performed with the standard Marquardt algorithm,[23] using one of two equations, depending on the experiment, and assuming a single exponential function for the sample excited state decay in both cases. For the case of identical pump and probe wavelengths, a symmetrical curve of intensity vs delay is obtained, and the following equation is used:

$$I(t)=\int_{-\infty}^{\infty} G(t')\exp(-|t-t'|/\tau)dt', \tag{1}$$

where $I(t)$ is the measured intensity curve (minus the base line), $G(t)$ is the measured cross-correlation curve, and τ is the S_1 lifetime of the sample. For the case in which the pump wavelength is less than the probe wavelength (such that the probe laser does not promote the $S_1 \leftarrow S_0$ transition), an unsymmetrical curve is obtained, and the following equation is used:

$$I(t)=\int_0^t G(t')\exp[-(t-t')/\tau]dt'. \tag{2}$$

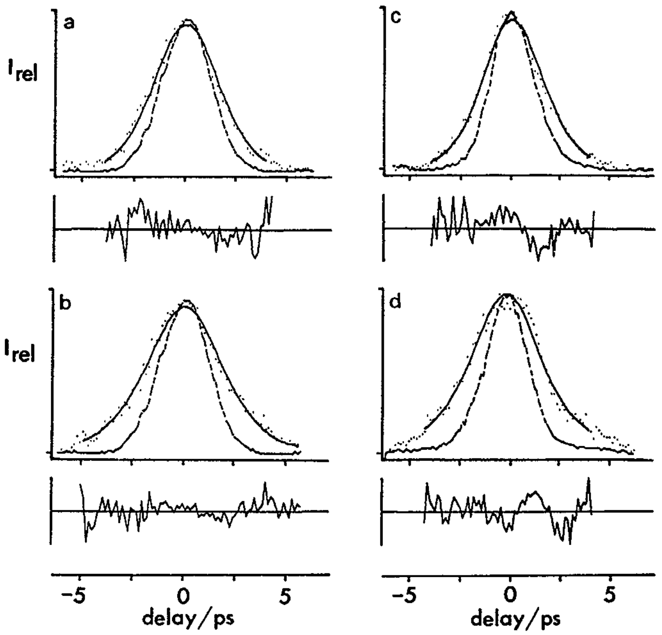

FIG. 2. Relative emission intensity vs relative delay time and plot of weighted residuals for (a) azulene in CH ($\tau=0.97$ ps); (b) azulene in MeCN ($\tau=1.48$ ps); (c) azulene-d_8 in CH ($\tau=0.96$ ps); and (d) azulene-d_8 in MeCN ($\tau=1.35$ ps). Pump and probe laser wavelengths at 685 nm; · · · sample emission; – – – αNPO emission; — fit to sample emission. The base line has been subtracted from the sample and αNPO data.

Although the fits were performed by minimizing the reduced χ^2,[23] the final χ^2 value thus obtained is not reflective of the quality of the fit. Since each data point is an average of ~10 intensity (cps) readings, the data are not Poisson-distributed (as it would be for a true single photon counting experiment[24]), and the value of the reduced χ^2 cannot be used to evaluate the fit. Hence, the goodness of fit was determined by visual inspection of the fit and the plot of weighted residuals.[23]

A typical αNPO peak has a FWHM of 2.5 ps. Since the dye laser pulses are typically 0.5 ps wide, most of the measured cross-correlation width arises from the relative jitter between the two trains of pulses. The cross-correlation FWHM can be related to the dye laser pulse widths and the relative temporal jitter between them by the following working expressions:

$$\mathrm{FWHM}^2_{\mathrm{CC}}=\mathrm{FWHM}^2_{\mathrm{DL1}}+\mathrm{FWHM}^2_{\mathrm{DL2}}+(\mathrm{jitter})^2, \tag{3}$$

where DL1 and DL2 refer to the two dye lasers. Solving this using typical FWHM data gives a jitter of 2.4 ps. A typical scan of an azulene sample has a peak:base line ratio of 1.8–2.0. The maximum intensity obtained from a 6×10^{-3} M solution of azulene was ~1700 cps (base line ~1000 cps). The emission intensity from αNPO was very high, and a 4×10^{-4} M solution was used to keep the peak count rate under 10 000 cps.

III. RESULTS AND DISCUSSION

Figure 2 shows the measured emission intensity and the instrument response function (two photon fluorescence

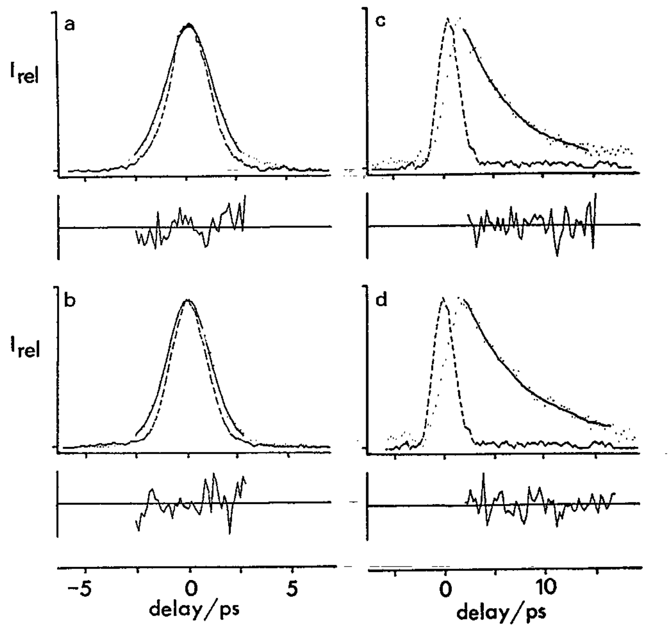

FIG. 3. Relative emission intensity vs relative delay time and plot of weighted residuals for (a) guaiazulene in CH (τ=0.58 ps); (b) guaiazulene in MeCN (τ=0.48 ps); (c) trimethylazulene in CH (τ=4.47 ps); and (d) trimethylazulene in MeCN (τ=5.69 ps). Pump and probe laser wavelengths at 685 nm for guaiazulene, 630 and 700 nm, respectively for trimethylazulene; · · · sample emission; --- αNPO emission; — fit to sample emission. The base line has been subtracted from the sample and αNPO data.

from αNPO) as a function of the relative time delay between pulses for AZ and AZ-d_8 in CH and MeCN. The pump and probe wavelengths are nominally the same (685 nm) in these experiments. However, because they are generated by two different dye lasers and because the jitter between the two trains of pulses is substantial, the coherence spike[12,13,17,18] observed when a single dye laser is used to produce both pump and probe beams is absent here.

Figure 3 shows the measured emission intensity as a function of relative time delay between the pulses for GAZ and TMA in CH and MeCN. For GAZ, the laser wavelengths were the same as those employed for AZ. However, in the case of TMA, different pump (630 nm) and probe (700 nm) wavelengths were used, since this compound does not exhibit measurable $S_1 \leftarrow S_0$ absorption at 685 nm (the central wavelength of overlap for the two laser dye tuning curves). The use of different pump and probe wavelengths leads to an unsymmetrical decay curve, because only the pump can promote the $S_1 \leftarrow S_0$ transition. The lifetimes of GAZ are slightly shorter, while those of TMA are significantly longer, than those of AZ and AZ-d_8. A significant solvent effect is again observed for TMA. In the case of GAZ, the S_1 lifetime is much shorter than the temporal width of the instrument response function, making accurate deconvolution difficult. The GAZ lifetimes therefore lie close to the time-resolving limit of this apparatus when it is used in the two laser, pump–probe mode. For this reason the relative error in these lifetimes is too large to permit an evaluation of a possible solvent effect in GAZ.

Table I summarizes the S_1 lifetime data, and also presents the measured S_1–S_0 electronic energy spacings and the values of the overall rate constants for the radiationless decay of S_1. The latter may be calculated accurately from $\Sigma k_{NR} = 1/\tau(S_1)$ because radiative decay contributes negligibly to the S_1 relaxation rate in all the systems examined here. Inspection of these data and comparison of them with previous work reveals the following:

(1) The lifetimes of AZ and AZ-d_8 in CH and TCE reported here are the same as those measured by Schwarzer *et al.*[17] under conditions which are identical other than excitation wavelength, λ_{ex} (685 nm vs 613 nm). These lifetimes are, however, significantly smaller than the oft-quoted value of 1.9±0.2 ps (for λ_{ex}=615 nm) which Ippen and co-workers[12,13] report is solvent-independent.

(2) The S_1 lifetimes of AZ, AZ-d_8, and TMA are significantly longer in acetonitrile, a polar solvent, than in the two nonpolar solvents, CH and TCE. The longer lifetimes correlate qualitatively with the larger S_1–S_0 energy gaps in the more polar solvents.

(3) The lifetimes of AZ and AZ-d_8 are identical within a small experimental error (~ ±10%) in a given polar or nonpolar solvent, in agreement with previous reports.[12,13,17] The deuterium isotope effect on S_1's nonradiative electronic relaxation, $\Sigma(k_{NR})_H/\Sigma(k_{NR})_D$, is therefore 1.0±0.1 for azulene itself in fluid solution.

TABLE I. Pump–probe results for the S_1 decay of azulene, azulene-d_8, and 4,6,8-trimethylazulene in several solvents at room temperature.

Compound	Solvent	$\Delta E(S_1\text{–}S_0)/$ 10^3 cm^{-1}	N^a_{meas}	τ_{av}/ps	$\Sigma k_{NR}/$ 10^{11} s^{-1}
guaiazulene	CH	13.72	4	0.56±0.13	17.8
	MeCN	13.90	5	0.44±0.10	22.7
azulene	CH	14.37	15	1.03±0.10	9.71
	TCE	14.40	7	1.02±0.13	9.80
	MeCN	14.66	6	1.42±0.07	7.04
azulene-d_8	CH	14.40	5	0.95±0.05	10.5
	MeCN	14.62	4	1.40±0.09	7.14
trimethyl-azulene	CH	15.53	6	4.0 ±0.3	2.50
	MeCN	15.90	4	5.6 ±0.1	1.78

[a] N_{meas} is the number of independent experiments performed in each case.

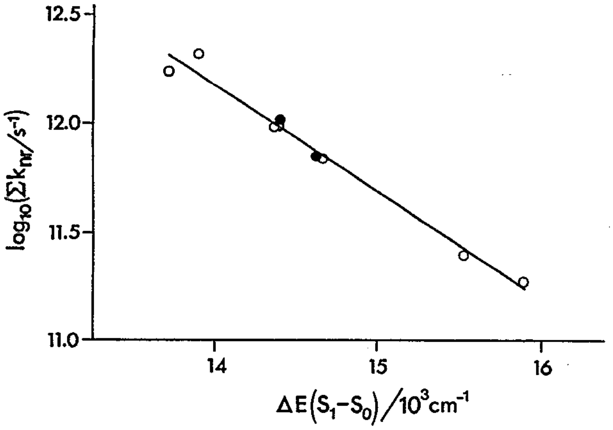

FIG. 4. Plot of log (Σk_{NR}) vs S_1–S_0 energy gap for azulene and derivatives in several solvents at room temperature. Line of best fit, slope$=-0.51\times10^{-3}$ cm; y-int$=19.3$; correlation$=0.989$. The filled symbols are for azulene-d_8.

(4) The lifetimes of AZ, GAZ, and TMA in a given solvent also increase with increasing S_1–S_0 energy gap.

The combined data for all four compounds in all three solvents are plotted in $\log_{10}(\Sigma k_{\mathrm{NR}})$ vs $\Delta E(S_1$–$S_0)$ form in Fig. 4. Despite the significantly larger relative error in the measured lifetimes of GAZ, the semilogarithmic correlation is excellent ($r=0.989$). This then leads us to consider interpreting the data in terms of the statistical limit case of radiationless transition theory[25] and the weak-coupling, "energy gap law" formalism developed by Englman and Jortner.[26]

In the weak-coupling, statistical limit case the rate constant for the radiationless decay of a large molecule is given by the Golden Rule expression,

$$k_{\mathrm{NR}}=\left(\frac{2\pi\rho}{\hbar}\right)\beta_{\mathrm{el}}^2F, \tag{4}$$

where ρ is the density of final states equiergic with a given initial state, β_{el} is the electronic matrix element which describes the coupling between the initial and final states, and F is the Franck–Condon factor for the transition. F is the sum of the squares of vibrational overlap functions of the form $\langle\chi_i/\chi_f\rangle$, where the χ are themselves products of N vibrational wave functions describing the normal modes of the molecule. Siebrand and others[25–28] have shown that when the electronic energy spacing, ΔE, is sufficiently large, F varies approximately exponentially with vibrational quantum number (v_f) of the energy accepting modes in the final state. The absolute magnitude of F, however, is determined not only by v_f, the accepting mode frequencies ($\hbar\omega_N$), and ΔE, but also by the displacement (change of equilibrium position) and distortion (change of shape) of the coupled vibrational potentials. The main contributors to F, i.e., the preferred accepting modes, are expected to be displaced oscillators at small ΔE and distorted oscillators at large ΔE,[27] and may be identified by determining those vibrations which exhibit the largest frequency changes between the two states.

The fact that the semilogarithmic plot of Fig. 4 yields a single straight line over the available 2200 cm^{-1} span of ΔE suggests that $S_1 \rightsquigarrow S_0^v$ internal conversion (IC), not intersystem crossing (ISC), is the principal radiationless relaxation process in the S_1 states of these compounds. Thus $\Sigma k_{\mathrm{NR}}=k_{\mathrm{IC}}\gg k_{\mathrm{ISC}}$, a conclusion which is now uniformly supported[9–19] notwithstanding an early report to the contrary.[8] The excellent energy gap law correlation also suggests that changes in F for the $S_1 \rightsquigarrow S_0^v$ internal conversion process are solely responsible for the observed variations in the nonradiative decay rates. Why the additional torsional states apparently do not enhance the rates of nonradiative decay of the alkyl-substituted compounds remains an open question.

Variations in ΔE and consequent variations in F brought about either by changing the polarity of the solvent or by introducing substituents on the azulene chromophore have the same effect on k_{IC}. Thus β_{el} appears to be the same for all four molecules, AZ, AZ-d_8, TMA, and GAZ, i.e., the substitution of alkyl groups has no effect other than that of modifying the electronic energy gap. Furthermore it appears to be immaterial whether the solvent is polar (acetonitrile), nonpolar (cyclohexane), or lacks high frequency C–H oscillators (TCE). That is, the structure of the solvent is irrelevant (at least for these nonviscous liquids at room temperature), and apart from the small modification of ΔE the medium acts as a classical inert heat bath.[29] Within the framework of the standard theory of radiationless transitions, such a medium is one which provides for efficient vibrational thermalization of a solute, but which itself does not significantly distort or displace the solute potential surfaces. In such a medium the electronic relaxation rate should not be a function of solvent structure for the same energy gap, a condition which is clearly fulfilled for AZ in CH and TCE. Furthermore, in an inert heat bath the nonradiative electronic relaxation rate from the origin should differ from that of the isolated molecule only by an amount related to the difference in ΔE between the solution and gas phase. Using absorption linewidth measurements Kulkarni and Kenny,[16] Amirav and Jortner,[14] and Suzuki and Ito[15] have shown that the lifetime of isolated AZ $S_1(v=0)$ lies between 1.1 and 0.8 ps. It is thus of interest to note that the value of k_{IC} for the $v=0$ level of the S_1 state of isolated azulene falls squarely on the line in Fig. 4 if the point is plotted at $\Delta E=14\,284$ cm^{-1}, the electronic origin of the S_1–S_0 transition in the gas phase.[15] In solution at room temperature azulene molecules will, on average, possess several hundred cm^{-1} of vibrational energy (disposed largely in the optically inactive, low frequency modes[15]). Moreover, the value of k_{IC} increases approximately linearly with increasing vibrational energy in the isolated molecule. Nevertheless, the observations that the medium appears to be "inert" and that $k_{\mathrm{IC}}(v=0)$ for isolated AZ falls on the solution phase energy gap correlation line suggest that $S_1 \rightsquigarrow S_0^v$ might occur preferentially from $v=0$ even when S_1 is in solution at room temperature. The implication of this suggestion is either that the population of low frequency optically inactive nontotally symmetric vibrational states in S_1 does not enhance the $S_1 \rightsquigarrow S_0^v$ radiationless decay rate or that vibrational relaxation and redistribution occur in solution on a time scale which is fast compared with the rate of electronic relaxation. Support is available for both suggestions (*vide infra*).

The present results are also consistent with the observation that the lifetime of the S_1 state of AZ is significantly longer ($\geqslant 3.3$ ps) in a naphthalene host[30] in liquid He than in either the isolated molecule or fluid solution. Based on Fig. 4 the value of $\tau(S_1)$ expected for AZ-h_8 in an inert medium in which $\Delta E = 14\,652\ \mathrm{cm}^{-1}$ (the S_1–S_0 gap in a naphthalene host[30]) should be ~ 1.4 ps. Amirav and Jortner[14] have suggested that this difference is due to "clamping" of the high amplitude, low frequency accepting modes of the azulene guest by the solid host. This suggestion is completely consistent with both spectroscopic evidence of the sensitivity of the frequency of mode 39 (C–C–C inplane bend of b_1 symmetry; the molecule lies in the xz plane) to the nature of the host environment,[15,30] and the present results which show that the increase in ΔE should contribute no more than 20% of the increase in $\tau(S_1)$ on proceeding from the cold isolated molecule to the naphthalene host at 1.2 K. The diminished importance of low frequency vibrations as accepting modes in the solid is also consistent with the observation of a small isotope effect $(k_{\mathrm{IC}})_{\mathrm{H}}/(k_{\mathrm{IC}})_{\mathrm{D}} = 1.27$, for AZ in solid naphthalene[30] compared with 1.0 ± 0.1 in fluid solution where vibrational clamping would be negligible.

The present results are also consistent with earlier suggestions[10–13,17] that the rate of vibrational relaxation of azulene in solution is considerably faster than its rate of electronic relaxation following $S_0 + h\nu \rightarrow S_1^v$ excitation, and that internal conversion occurs from the equilibrated S_1 state irrespective of λ_{ex}. Thus $\tau(S_1)$ for azulene in a given solvent (CH or TCE) is the same for excitation at $\lambda_{\mathrm{ex}} = 613$ nm (Ref. 17) or 685 nm where the initial excess vibrational energy in S_1, $E_{\mathrm{vib}}^{\mathrm{ex}}$ ranges from $\sim 1900\ \mathrm{cm}^{-1}$ to $\sim 230\ \mathrm{cm}^{-1}$, respectively. Recent direct measurements give values of the vibrational relaxation times of the first excited singlet state of azulene in ethylene glycol of 50 fs at 617 nm to 300 fs at 648 nm,[18] and confirm this suggestion. Note, however, that the electronic relaxation time measured in the same study,[30] 3.0 ps independent of λ_{ex}, appears to be unusually long even for a polar, viscous fluid medium.

Finally we address the question of the nature of the preferred accepting modes in the $S_1 \rightsquigarrow S_0^v$ process. The complete absence of a measurable deuterium isotope effect suggests that, unlike the alternant aromatic hydrocarbons,[28] high frequency in-plane C–H(D) stretching vibrations are not important accepting modes for azulene and its derivatives in solution. By default this suggests that lower frequency oscillators which suffer the greatest distortion and/or displacement must be involved. Only nine a, and two b, vibrations are optically active in the $S_1 \leftarrow S_0$ spectrum[15] and only one of these, mode 39 (C–C–C bend), undergoes a frequency change of more than 6%.[15,31,32] However, from an examination of the S_2–S_0 spectra of azulene vapor in a bulb at room temperature, Ito and co-workers[15,31] conclude that many low frequency out-of-plane C–C–C bending modes (three of a_2 symmetry and four of b_2 symmetry[32]) also undergo substantial frequency changes between S_0 and S_1 or S_2.

Thus the simple energy gap law formalism developed by Englman, Jortner, and Freed[26,29] cannot be applied directly to the radiationless relaxation of azulene in its S_1 state. Physically meaningful results are not obtained when the slope of Fig. 4, -0.51×10^{-3} cm, is used together with any of the low frequency vibrations to calculate values of the exponential parameter, $\gamma = \ln(2\Delta E/\Sigma\hbar\omega\Delta^2) - 1$, from the energy gap law.[26]

IV. CONCLUSIONS

A significant solvent effect has been observed on the S_1 lifetime of azulene and three of its derivatives using a pump–probe technique with subpicosecond resolution. The rate constants for the radiationless relaxation of S_1 of all four compounds in three solvents of different structure and polarity all exhibit the same "energy gap law" correlation with $\Delta E(S_1$–$S_0)$. From this we conclude that the changes in the rates of internal conversion of the S_1 states are governed exclusively by changes in the Franck–Condon factors for the transitions, and that both solvent-induced and substituent-induced shifts in ΔE operate in the same fashion in this respect. Because k_{IC} is the same in solvents having the same ΔE but different structure and because the value of k_{IC} for isolated vibrationless azulene also correlates well with the solution phase data, we conclude that the solvent is acting as a classical heat bath in our experiments.

Changing the excitation wavelength, and hence the initial excess vibrational energy in S_1, has no effect on the electronic relaxation rate for $E_{\mathrm{vib}}^{\mathrm{ex}}$ up to at least $\sim 2000\ \mathrm{cm}^{-1}$. We conclude that vibrational relaxation occurs on a time scale which is fast in comparison with that of electronic relaxation, so that S_1 decays from an equilibrated ensemble of molecules in these fluid solutions at room temperature.

Finally, in agreement with previous suggestions, we conclude from a measurement of the deuterium isotope effect of 1.0 ± 0.1 that the radiationless decay of azulene S_1 does not involve high energy C–H(D) stretching vibrations as accepting modes to a significant extent.

ACKNOWLEDGMENTS

We are grateful to Dr. Bernhard Nickel, Max–Planck Institut für Biophysikalische Chemie, Göttingen, for supplying purified samples of azulene and azulene-d_8, and to Mr. Dietrich Tittelbach-Helmrich for synthesizing the 4,6,8-trimethylazulene. The research was made possible by a grant funded by the Network of Centers of Excellence Program in association with the Natural Sciences and Engineering Research Council of Canada (NSERCC) and by a NSERCC operating Grant. B. D. W. gratefully acknowledges the award of a NSERCC Postdoctoral Fellowship.

[1] M. Beer and H. C. Longuet-Higgins, J. Chem. Phys. **23**, 1390 (1955).

[2] G. Viswanath and M. Kasha, J. Chem. Phys. **24**, 574 (1956).

[3] T. M. Woudenberg, S. K. Kulkarni, and J. E. Kenny, J. Chem. Phys. **89**, 2789 (1988).

[4] D. R. Demmer, J. W. Hager, G. W. Leach, and S. C. Wallace, Chem. Phys. Lett. **136**, 329 (1987).

[5] B. D. Wagner, D. Tittelbach-Helmrich, and R. P. Steer, J. Phys. Chem. **96**, 7904 (1992).

[6] P. M. Rentzepis, Chem. Phys. Lett. **2**, 117 (1968).

[7] *Ultrafast Phenomena, VI*, Springer-Verlag Series in Chemical Physics, edited by T. Yajima, K. Yoshihara, C. B. Harris, and S. Shionaya (Springer, Berlin, 1988), Vol. 48.

[8] E. Drent, G. M. van der Deijl, and P. J. Zandstra, Chem. Phys. Lett. **2**, 526 (1968).

[9] R. M. Hochstrasser and T.-Y. Li, J. Mol. Spectrosc. **41**, 297 (1972).

[10] P. Wirth, S. Schneider, and F. Dörr, Chem. Phys. Lett. **42**, 482 (1976).

[11] J. P. Heritage and A. Penzkofer, Chem. Phys. Lett. **44**, 76 (1976).

[12] E. P. Ippen, C. V. Shank, and R. L. Woerner, Chem. Phys. Lett. **46**, 20 (1977).

[13] C. V. Shank, E. P. Ippen, O. Teschke, and R. L. Fork, Chem. Phys. Lett. **57**, 433 (1978).

[14] A. Amirav and J. Jortner, J. Chem. Phys. **81**, 4200 (1984).

[15] T. Suzuki and M. Ito, J. Phys. Chem. **91**, 3537 (1987).

[16] S. K. Kulkarni and J. E. Kenny, J. Chem. Phys. **89**, 4441 (1988).

[17] D. Schwarzer, J. Troe, and J. Schroeder, Ber. Bunsenges. Phys. Chem. **95**, 933 (1991).

[18] T. Matsumoto, K. Ueda, and M. Tomita, Chem. Phys. Lett. **191**, 627 (1992).

[19] A. L. Sobolewski, Chem. Phys. **115**, 469 (1987).

[20] M. E. Garst, J. Hochlowski, J. G. Douglas III, and S. Sasse, J. Chem. Ed. **60**, 511 (1983).

[21] A. M. Johnson and W. M. Simpson, J. Opt. Soc. Am. B **2**, 619 (1985).

[22] K. L. Sala, G. A. Kenney-Wallace, and G. E. Hall, IEEE J. Quantum Electron. **QE-16**, 990 (1980).

[23] P. R. Bevington, *Data Reduction and Error Analysis for the Physical Sciences* (McGraw–Hill, New York, 1969).

[24] D. V. O'Connor and D. Phillips, *Time-Correlated Single Photon Counting* (Academic, London, 1984).

[25] P. Avouris, W. M. Gelbart, and M. A. El-Sayed, Chem. Rev. **77**, 793 (1977).

[26] R. Englman and J. Jortner, Mol. Phys. **18**, 145 (1970).

[27] W. Siebrand, J. Chem. Phys. **46**, 440 (1967).

[28] W. Siebrand and D. F. Williams, J. Chem. Phys. **49**, 1860 (1968).

[29] K. F. Freed and J. Jortner, J. Chem. Phys. **52**, 6272 (1970).

[30] R. M. Hochstrasser and T.-Y. Li, J. Mol. Spectrosc. **41**, 297 (1972).

[31] M. Fujii, T. Ebata, N. Mekami, and M. Ito, Chem. Phys. **77**, 191 (1983).

[32] R. S. Chao and R. K. Khanna, Spectrochim. Acta **33A**, 53 (1977).

The Journal of Chemical Physics is copyrighted by the American Institute of Physics (AIP). Redistribution of journal material is subject to the AIP online journal license and/or AIP copyright. For more information, see http://ojps.aip.org/jcpo/jcpcr/jsp
Copyright of Journal of Chemical Physics is the property of American Institute of Physics and its content may not be copied or emailed to multiple sites or posted to a listserv without the copyright holder's express written permission. However, users may print, download, or email articles for individual use.

The Journal of Chemical Physics is copyrighted by the American Institute of Physics (AIP). Redistribution of journal material is subject to the AIP online journal license and/or AIP copyright. For more information, see http://ojps.aip.org/jcpo/jcpcr/jsp